



INTERNATIONAL ATOMIC ENERGY AGENCY  
UNITED NATIONS EDUCATIONAL, SCIENTIFIC AND CULTURAL ORGANIZATION  
**INTERNATIONAL CENTRE FOR THEORETICAL PHYSICS**  
I.C.T.P., P.O. BOX 586, 34100 TRIESTE, ITALY, CABLE: CENTRATOM TRIESTE



UNITED NATIONS INDUSTRIAL DEVELOPMENT ORGANIZATION



**INTERNATIONAL CENTRE FOR SCIENCE AND HIGH TECHNOLOGY**

INTERNATIONAL CENTRE FOR THEORETICAL PHYSICS, 34100 TRIESTE (ITALY) VIA CARLINO, 41 ANDRINICO-PALACE P.O. BOX 586 TELEPHONE 0423571111 FAX 0423571111 TELETYPE 0423571111

SMR.550 - 3

**SPRING COLLEGE IN MATERIALS SCIENCE ON  
"NUCLEATION, GROWTH AND SEGREGATION IN MATERIALS  
SCIENCE AND ENGINEERING"  
( 6 May - 7 June 1991 )**

**SCANNING ELECTRON MICROSCOPY AND SCANNING  
TRANSMISSION ELECTRON MICROSCOPY**

**M.L. JENKINS**  
Department of Materials  
University of Oxford  
Parks Road  
Oxford OX1 3PH  
United Kingdom

Scanning electron microscopy and scanning transmission electron microscopy

M L Jenkins

I am grateful to Professor F J Humphreys and Dr N L Long for permission to use lecture notes prepared by them. Other notes are taken from 'A guide to energy-dispersive X-ray analysis' provided by Link Systems plc.

These are preliminary lecture notes, intended only for distribution to participants.

M L Jenkins

## The Scanning Electron Microscopy (3 lectures)

1. How it works
2. Obtaining a signal in the SEM
3. The optics of the SEM
4. The performance of the SEM
5. The ultimate resolution of the SEM
6. Topographical images
7. Backscattered electrons
8. The use of other signals in the SEM
9. Image acquisition, processing and storage

## The Scanning Transmission Electron Microscope (2 lectures)

1. The STEM: Analytical TEMs and dedicated FEGSTEMs
2. X-ray microanalysis in the STEM
3. Electron energy loss spectroscopy (EELS)
4. Light element analysis

## 1. HOW IT WORKS

The scanning electron microscope (SEM) is similar to the transmission electron microscope (TEM) in that they both employ a beam of electrons directed at the specimen. This means that certain features, such as the electron gun, condenser lenses and vacuum system, are similar in both instruments. However, the ways in which the images are produced and magnified are entirely different, and whereas the TEM provides information about the internal structure of thin specimens, the SEM is primarily used to study the surface, or near surface structure of bulk specimens.

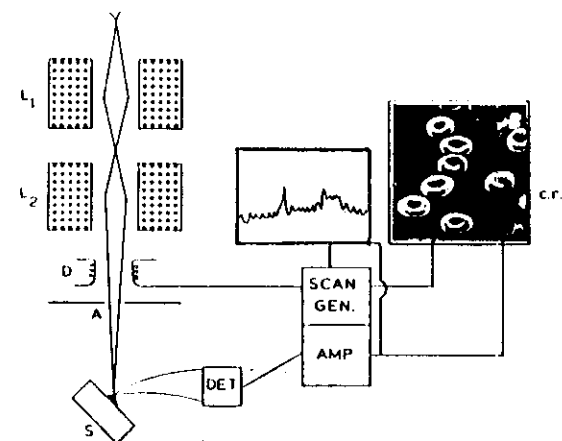


Fig 1. Schematic diagram of an SEM.

An electron gun, usually of the tungsten filament thermionic emission type produces electrons, and accelerates them to an energy between about 2 keV and 40 keV, rather lower than typical TEM energies (80-200 keV). Two or three condenser lenses then demagnify the electron beam until, as it hits the specimen, it may have a diameter of only 2-10 nm.

The fine beam of electrons is scanned across the specimen by the deflector coils, while a detector counts the number of low energy secondary electrons, or other radiation, given off from each point on the surface. At the same time, the spot of a cathode ray tube (c.r.t.) is scanned across the screen, while the brightness of the spot is modulated by the amplified current from the detector. The electron beam and the c.r.t. spot are both scanned in a similar way to a television receiver, that is, in a rectangular set of straight lines known as a raster. The mechanism by which the image is magnified is then extremely simple and involves no lenses at all. The raster scanned by the electron beam on the specimen is made smaller than the raster displayed on the c.r.t. The linear magnification is then the side length of the c.r.t. (L) divided by the side length (l) of the raster on the specimen (fig. 2a).

For example, if the electron beam is made to scan a raster 10µm x 10µm on the specimen, and the image is displayed on a c.r.t. screen 100mm x 100 mm, the linear magnification will be 10000x. Alternatively, or sometimes simultaneously on a separate waveform monitor, the microscope can display the variation of signal with beam position for the current raster line, as shown in figure 1.

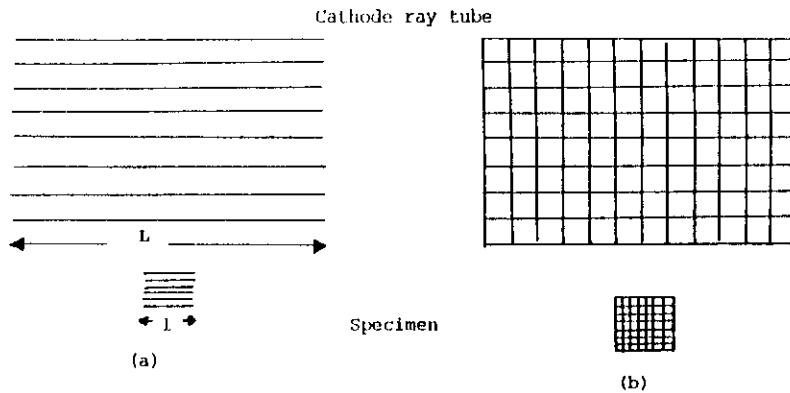


Fig 2. a) The rasters on the specimen and c.r.t. b) The equivalent pixels.

## 2. OBTAINING A SIGNAL IN THE SEM

One of the main features of the SEM is that, in principle, any radiation from the specimen or any measurable change in the specimen may be used to provide the signal to modulate the c.r.t. and thus provide contrast in the image. Each signal is the result of some particular interaction between the incident electrons and the specimen, and may provide us with different information about the specimen.

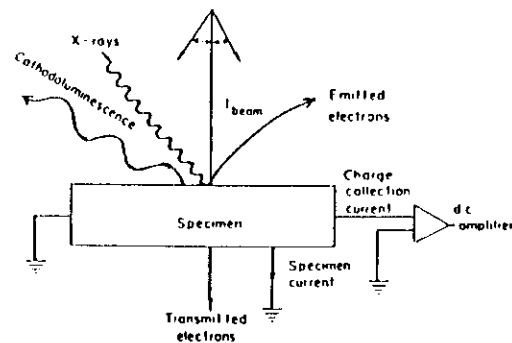


Fig 3. the origin of signals in the SEM

All scanning electron microscopes normally have facilities for detecting secondary electrons and backscattered electrons. Of the other radiations, x-rays are used primarily for chemical analysis rather than imaging. Auger electrons are of such low energy, and are so easily absorbed that they require an ultra high vacuum system and specialised equipment for their efficient use. Monte Carlo simulations and also direct experiments, have shown that the electrons are scattered in the specimen within a region such as that shown in figure 4.

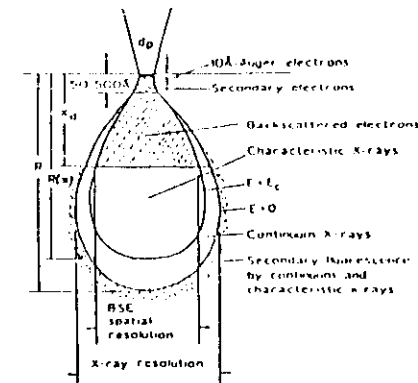


Figure 4. Interaction and sampling volumes for some radiations.

The region into which the electrons penetrate the specimen is known as the **interaction volume**, and throughout it, the various radiations are generated as a result of inelastic scattering, although as the primary electrons lose energy, the amount and type of the secondary radiations will alter.

Even though a secondary radiation is generated within this volume, it will not be detected unless it escapes from the specimen, and this will depend on the radiation and the specimen. Thus, x-rays are not easily absorbed, and most will escape from the specimen. Therefore the volume of material contributing to the x-ray signal, or **sampling volume**, is of the same order as the interaction volume, which may be several microns in diameter. Electrons will not be backscattered out of the specimen if they have penetrated more than a fraction of a micron, and they therefore originate from a much smaller region as shown in figure 4. Although secondary electrons are generated both by the primary electrons entering the specimen and by the escaping backscattered electrons, the former are more numerous, and therefore the detected secondary electron signal originates mainly from a region which is little larger than the diameter of the incident beam, as shown schematically in figure 5

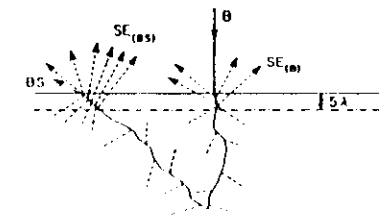


Figure 5. Secondary electron generation.

The numbers of secondary and backscattered electrons emitted from the specimen for each incident electron are known as the **secondary electron coefficient ( $\delta$ )** and the **backscattered electron coefficient ( $\eta$ )** respectively.

By far the most widely used signal in the scanning electron microscope is that

from secondary electrons. Secondary electrons are detected by a scintillator - photomultiplier system known as the Everhart-Thornley detector.

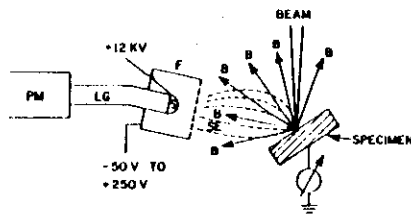


Figure 6. The Everhart Thornley secondary electron detector.

The secondary electrons strike a scintillator, e.g. a phosphor, which then emits light. The light is transmitted through a light pipe, and into a photomultiplier which converts the photons into pulses of electrons, which may then be amplified and used to modulate the intensity of the c.r.t.

The energy of the secondary electrons (10-50eV) is too low to excite the scintillator, and so they are first accelerated by applying a bias voltage of +10keV to a thin aluminium film covering the scintillator. A metal grid or collector, at a potential of several hundred volts surrounds the scintillator, and this has two purposes. Firstly it prevents the high voltage of the scintillator affecting the incident electron beam, and secondly, it improves the collection efficiency by attracting secondary electrons, and thus collecting even those which were initially not moving towards the detector. The Everhart-Thornley detector system is very efficient, and for flat specimens, almost all the secondary electrons are collected.

### 3 THE OPTICS OF THE SEM

The purpose of the lenses in the SEM is to produce a fine beam of electrons incident on the specimen. Figure 7 is a simplified ray diagram of a microscope which has two lenses, a condenser lens, and an objective lens. We can understand the main features of the microscope by treating the electromagnetic lenses as thin convex optical lenses, and using geometric optics theory. For the moment, we will ignore lens defects.

The electron gun produces a monochromatic beam of electrons, with a current in the beam of  $B$ . The condenser lens, of focal length  $F_c$ , collects most of these electrons and produces a demagnified image of the filament at a distance  $V_1$  from the condenser lens. If the diameter of the filament is  $D_0$ , then the diameter of the intermediate filament image ( $D_1$ ) is given by :-

$$D_1 = D_0 \times V_1/U_1 \quad 1$$

The objective lens, of focal length  $F_o$ , is used to further demagnify the filament image, producing a probe, of diameter  $D$  on the surface of the specimen, which is a distance  $V_2$  below the objective lens. The distance  $V_2$  is known as the working distance ( $WD$ ) of the microscope.

The diameter of the final probe on the specimen is then :-

$$D = D_1 \times V_2/U_2 = D_1 \times WD/U_2 \quad 2$$

It can be seen that if the focal length of the condenser lens is increased,  $V_1$

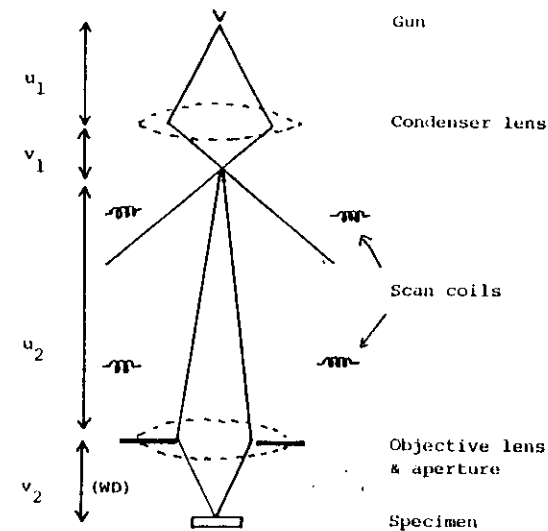


Figure 7. Ray diagram of SEM

decreases, and the intermediate beam diameter  $D_1$  decreases.  $U_2$  must also increase, as  $U_2 + V_1$  is constant, and therefore the demagnification of the objective also increases, and the probe diameter decreases. The probe size in the SEM is therefore regulated by altering the strength of the condenser lens. For a constant condenser lens setting, equation 2 shows that the probe diameter also decreases as the working distance is decreased.

In order to minimise spherical aberration, the entry of rays into the objective lens is restricted by an aperture of diameter  $A$ , and therefore, as may be seen from figure 7, not all of the electron beam which passes through the condenser lens can enter the objective lens. If the semiangle of the rays leaving the condenser lens is  $(\alpha_0)$ , and the semiangle of the rays entering the objective lens is  $(\alpha_1)$ , then the current in the final probe is -

$$B_1 = B \times (\alpha_1/\alpha_0)^2 \quad 3$$

The current therefore decreases as the condenser lens strength increases (i.e. as the probe becomes smaller), and also decreases as the aperture diameter ( $A$ ) is reduced.

When we come to consider the ultimate resolution of the SEM, we will find that the probe size, and the current in the probe play important roles in determining the performance of the microscope.

Deflection of the beam is accomplished by energising a pair of coils as shown schematically in figure 8. In order to scan a raster, two orthogonal pairs of coils are required.

The SEM normally has two such sets of coils, which are set to deflect the beam in opposite directions. Thus, as seen in figure 8, the beam scans across the specimen, but always passes through the optic axis at the objective lens.

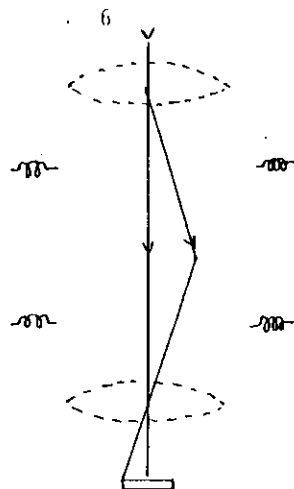


Figure 8. Movement of the axial ray during scanning.

#### 4. THE PERFORMANCE OF THE SEM

**4.1 Pixels.** The process of image formation in the scanning electron microscope is quite unlike the formation of an image in the optical or transmission electron microscope, as the image is built up sequentially during the scan. A very useful concept in understanding the imaging performance of the SEM is that of the picture element or pixel. The amplified signal from the detector is output to a high quality cathode ray tube, and the minimum size of spot which may be obtained on such a c.r.t. is typically about 0.1mm. A 100mm square c.r.t. can therefore contain 1000 x 1000 discrete picture points or pixels. These pixels are the fundamental units of the image, and can be considered as squares of diameter 0.1 mm with a uniform intensity and no internal structure. As shown in figure 2, the spot on the c.r.t. mimics the movement of the electron beam on the specimen, and therefore for each of the pixels on the c.r.t. there is a corresponding pixel on the specimen (fig.2b). The size of the specimen pixel (p) is given by :-

$$p = 100\mu\text{m} / M$$

4

Where M is the magnification.

We define the resolution as the smallest separation of two points which the microscope can detect as separate entities. It is clear that in order to resolve two features, e.g. A and B in figure 2b, they must occupy separate pixels. Therefore, the working resolution of the instrument can be no better than the specimen pixel size (p) as given by equation 1.

The size of the electron probe relative to the specimen pixel size is very important. If the electron probe is larger than the specimen pixel (fig.9a), then the signal from adjacent pixels is merged, and the resolution is degraded. If the electron probe is smaller than the specimen pixel (fig. 9b) then the signal will be weaker, and, as we will discuss later, may be noisy. It is clear that for optimum performance of the instrument, we should in general, aim to make the probe diameter (or more correctly the sampling volume) equal to the specimen pixel diameter. (fig. 9c). This means that for optimum performance, the probe size should be adjusted as the magnification of the microscope is altered.

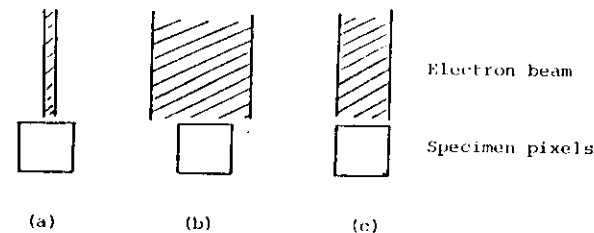


Figure 9. Relationship of specimen pixel size and probe size.

#### 4.2 Depth of field.

One of the most important aspects of the scanning electron microscope is its large depth of field.

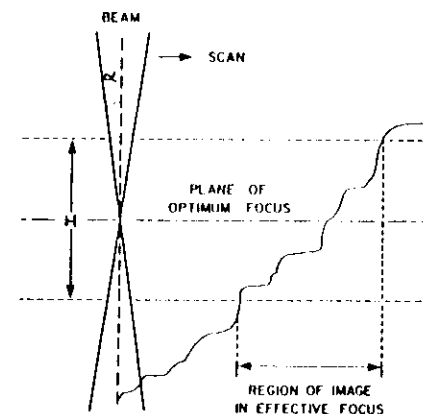


Figure 10. Depth of field in the SEM.

Figure 10 shows the electron beam emerging from the objective aperture and incident on a specimen. Although the beam is focussed on the specimen, the convergence angle ( $\alpha$ ) is small, and, assuming a point focus, the beam diameter defocusses by less than s over a vertical distance of H, where :-

$$s = H \alpha$$

5

If the defocus is no greater than a specimen pixel, then the image will remain in focus, and thus from equations 4 and 5 the distance H over which the specimen will remain in focus, the depth of field, is given by :-

$$H = \frac{0.1 \text{ mm}}{M \alpha}$$

6

From fig. 10 we see that the convergence angle  $\alpha$  of the beam is given by :-

$$\alpha = \frac{A}{2 WD} \quad 7$$

Thus from equations 6 and 7, we find that the depth of field is :-

$$H = \frac{0.2 WD}{A M} \quad 8$$

## 5. THE ULTIMATE RESOLUTION OF THE SEM

We saw in the last section that the best working resolution of the SEM, was the specimen pixel size (p), given by equation 4, and that this depended on the magnification of the instrument. However, this resolution is only achieved if the diameter of the beam sampling volume is no larger than p. No matter how good our microscope is, or how well we adjust it, we cannot achieve a spatial resolution which is better than this. Secondary electrons have the smallest sampling volume, with a diameter little larger than the probe diameter.

However, as the probe diameter is reduced, the beam current is decreased, and ultimately the beam current will be insufficient to generate a useable signal. Thus we can define the ultimate resolution of the SEM as being that of the smallest probe which can provide an adequate signal from the specimen.

### 5.1 The minimum attainable probe size.

The probe size may be decreased by increasing the strength of the condenser lens, and decreasing the working distance. As the latter occurs, the beam convergence angle ( $\alpha$ ) increases (fig. 10). Rays which are off the optic axis are subject to spherical aberration, and instead of a point focus on the specimen, we obtain a disc of diameter  $D_s$ , where :-

$$D_s = \frac{1}{2} C_s \alpha^3 \quad 9$$

Where  $C_s$  is the coefficient of spherical aberration of the lens.

There is also aberration introduced by diffraction at the aperture, which produces a minimum spot size of :-

$$D_d = 1.22 \lambda / \alpha \quad 10$$

Where  $\alpha$  is the electron wavelength.

If the microscope is adjusted so as to give a probe of theoretical diameter  $D_t$ , according to equation 2, then this value will be increased by the aberrations  $D_s$  and  $D_d$ . The real probe diameter (D) may be taken as :-

$$D = \sqrt{D_t^2 + D_s^2 + D_d^2} \quad 11$$

The minimum value of D, corresponding to the case when  $D_t = 0$ , is obtained by minimising the aberrations, and is given by :-

$$D_{min} = 1.29 \lambda^{3/4} C_s^{1/4} \quad 12$$

For a typical SEM, operating at 20 keV, with an objective lens of  $C_s = 20\text{mm}$ ,  $D_{min}$  is 2.3nm, and  $\alpha = 5.1 \times 10^{-3}$  radians.)

As discussed in section 3, as the probe diameter (D) is decreased, so the current (I) in the beam decreases. The relationship between these parameters is given by Pease and Nixon, for a thermionic emission filament, as :-

$$D = D_{min} \left[ \left( \frac{I}{j} \right) \times 10^9 + 1 \right]^{3/8} \quad 13$$

Where I = filament temperature

j = current density at the filament surface

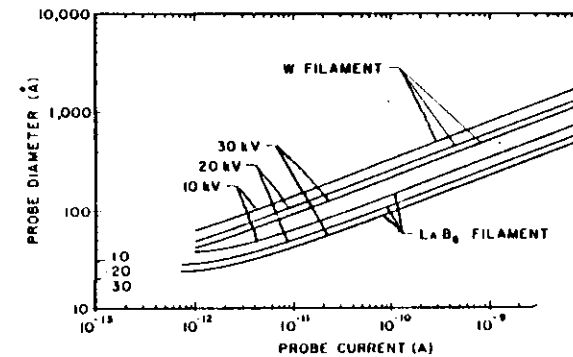


Figure 11. Relation between probe current and diameter.

### 5.2 The minimum useable current

In order to resolve two points on the specimen, there must be a discernible difference between the signals from these two regions.

Figure 12a shows the intrinsic signal from the specimen might vary with scan position. If we compare the signal  $S_{max}$  from one point of the specimen, with the signal  $S$  from an adjacent point, then the contrast from the specimen (C), sometimes called the **natural contrast**, is defined as :-

$$C = \frac{(S_{max} - S)}{S_{max}} = \frac{\Delta S}{S_{max}} \quad 14$$

Now the signal that is detected in the SEM is not a continuous signal, but for each pixel is derived from the number of secondary electrons ( $n$ ) arriving at the detector in a fixed time period. Because these events are randomly distributed in time, simple statistical theory tells us that if the average number of electrons detected from a particular point on the specimen is  $\bar{n}$ , then  $n$  will vary by an amount up to  $\sqrt{\bar{n}}$  about the mean. The noise (N) is then defined as  $\frac{\sqrt{\bar{n}}}{\bar{n}}$ .

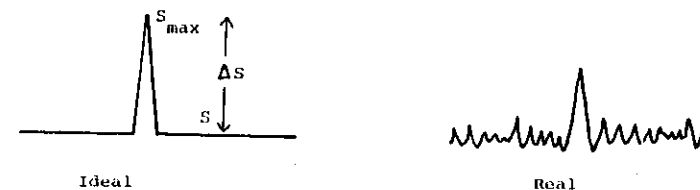


Figure 12. The effect of noise on the signal.

In a real situation therefore, the variation of signal with scan position will be as shown in figure 12b, with the noise tending to obscure the natural contrast of the specimen. Whether or not the observer can detect the two points of interest, i.e. whether they can see the contrast, is a physiological problem.

Rose has determined that the human eye can only distinguish two points on a c.r.t. if :-

$$S > 5N \quad \text{or} \quad \Delta S > 5\sqrt{n} \quad 15$$

We can use this criterion to determine the minimum level of contrast that can be observed. Combining equations 14 and 15, we find that the minimum level of contrast which can be observed is given by :-

$$C > 5 / \sqrt{n} \quad 16$$

The minimum level of signal necessary for us to observe a contrast level of  $C$  in the specimen is :-

$$\bar{n} > (5/C)^2 \quad 17$$

We can relate  $\bar{n}$ , the mean number of electrons detected for each pixel to the operating conditions of a microscope with a beam current  $I$ , and a frame scan time  $F$ .

The time ( $t$ ) that the beam dwells on a particular pixel is  $F \times 10^{-6}$ , if we assume, as before that we have  $10^6$  pixels in a frame. The number of electrons (of charge  $e$ ) which enter the specimen in this time is therefore :-

$$n_0 = I t / e = I F \times 10^{-6} / e \quad 18$$

The number of electrons actually detected ( $n$ ) will depend on the beam - specimen interaction, and the efficiency of the detector. We can write :-

$$n = q n_0 \quad 19$$

where  $q$  is the product of the detector efficiency and the electron yield. For secondary electrons, the former is approximately unity, and the latter is 0.1 - 0.2, giving a value for  $q$  of between 0.1 to 0.2.

By combining equations 17, 18 and 19, and putting  $e = 1.6 \times 10^{-19}$  coulombs, we can now express the Rose criterion in terms of the critical current ( $I_c$ ), which is required to discern a contrast level  $C$  in the specimen :-

$$I_c > \frac{4 \times 10^{-12}}{q F C^2} \quad \text{Amps} \quad 20$$

We can see from this equation that for a given detection system, there is a minimum beam current required to observe a particular contrast level, and that this current increases as the frame scan time decreases.

If we substitute  $I_c$  obtained from equation 20 into equation 13, then we can predict the minimum probe size, and therefore the best resolution obtainable in terms of a given contrast level in the specimen. This is shown graphically in figure 13, for a typical SLM using secondary electrons. The effect of frame scan time ( $F$ ) is also shown, for  $F$  varying between 100 seconds, which is a realistic value for photographic recording, and 0.02 seconds, which is the TV scan rate. (In constructing this graph, the following parameters have been assumed :-  $q = 0.2$ ,  $j = 4 \text{ A/cm}^2$ ,  $T = 2800\text{K}$ ,  $C_s = 20\text{nm}$ ,  $E = 20 \text{ keV}$ .)

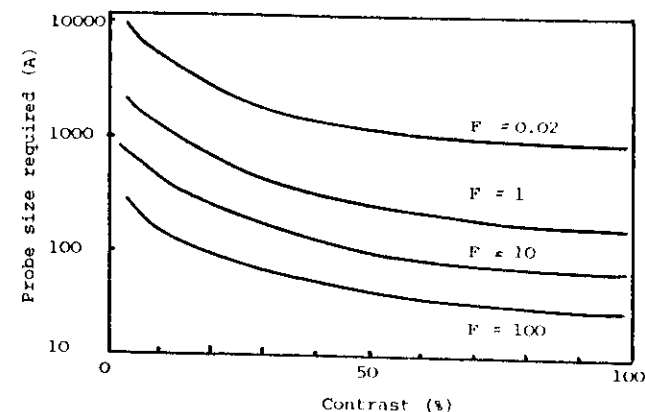


Figure 13. Minimum useable probe size as function of contrast and scan rate.

## 6. TOPOGRAPHIC IMAGES

One of the principal uses of the scanning electron microscope is to study the surface features, or **topography** of a sample. The discussion in the previous sections has shown that in order to obtain an image in the microscope, we must have some variation in the signal obtained from different parts of the specimen. Although topographic images may be obtained using most signals, we will only consider the use of secondary and backscattered electrons. The backscattered electron coefficient ( $\eta$ ) and the secondary electron coefficient ( $\delta$ ), are both a minimum when the surface of the specimen is perpendicular to the electron beam. This is because of the shape of the interaction volume and its relationship to the surface of the specimen, as shown schematically in figure 14. As the specimen is tilted, electrons are increasingly likely to be scattered out of the specimen, rather than further into the specimen.

The secondary electron coefficient varies with the tilt of the specimen ( $\theta$ ), as  $\delta = \delta_0 \sec \theta$ . Therefore, more secondaries are produced from tilted regions of the specimen. As the efficiency of the Everhart - Thornley detector is not very sensitive to the trajectories of the secondary electrons, we expect the number of detected electrons to therefore increase with surface tilt. It is for this reason that specimens being studied for topographic contrast with the ET detector are usually tilted some 20 - 40 degrees towards the detector (figure 6). Topographic images obtained with secondary electrons look remarkably like images of solid objects viewed with light. As we are accustomed to this sort of image, we find these topographic images easy to interpret. This similarity arises because of the very strong analogy between the two imaging modes.

In figure 15 light is arriving from almost all directions so that whatever the orientation of each of the facets A, B and C some light is reflected towards the eye. Figure 6 shows the analogous situation for secondary electrons in the SEM.

The only major difference is that the electrons are travelling in the opposite direction to the light rays. In fact there is a quantitative similarity between the two cases, as the intensity of diffusely reflected light is given by Lambert's law as being proportional to the cosine of the scattering angle. This is the inverse of the variation of  $\delta$  with tilt angle, and thus the analogy is exact. The specimen in the SEM therefore appears as if we were looking at it from above, when it is being illuminated with diffuse light, the detector being the source of the diffuse light.

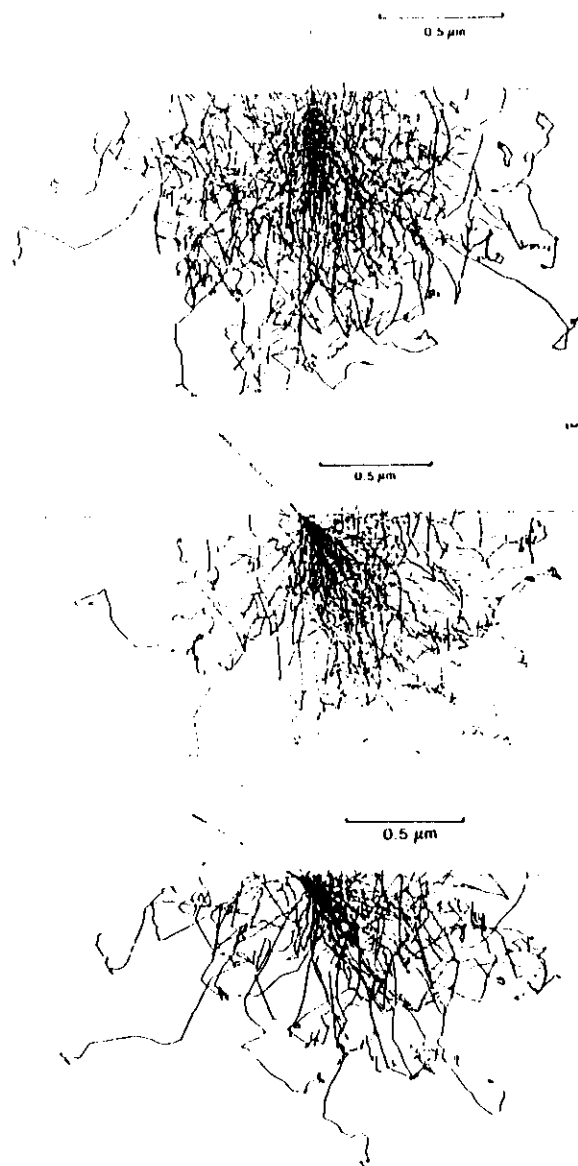


Figure 14. Effect of specimen tilt on interaction volume.

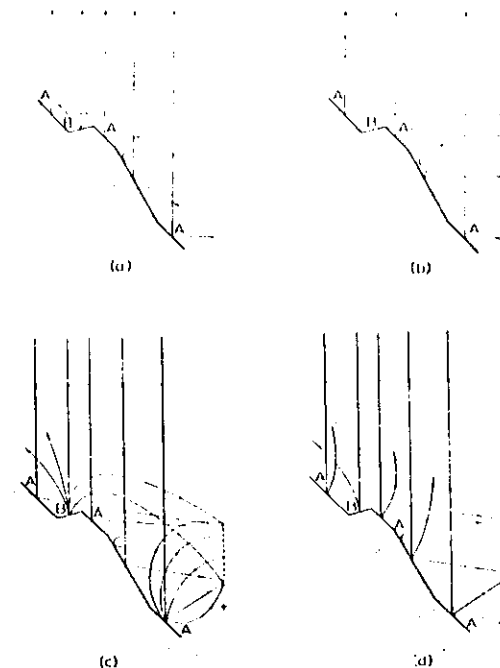


Figure 15. The analogy between the eye and the SEM. a) Diffuse illumination, viewed by eye. b) direct illumination viewed by eye. c) secondary electrons. d) backscattered electrons.

## 7. BACKSCATTERED ELECTRONS

### 7.1 Detecting backscattered electrons

Scintillator detectors. These detectors are of the scintillator-light pipe-photomultiplier type, and are designed to maximise the solid angle of collection. A good example of this is the Robinson detector shown schematically in figure 16a. The advantage of these detectors is their rapid response time, which means that, like the Everhart-Thornley detector, they may be used in conjunction with rapid scan rates. However, they are bulky, and may restrict the working distance of the microscope, and may need to be retracted if, for example, it is necessary to detect x-rays.

Solid State Detectors. When a high energy electron impinges on a semiconductor, it produces many electron-hole pairs. Normally these will rapidly recombine, but if a voltage is applied to the semiconductor, for example, by the self-bias generated by a p-n junction, then they may be separated, thus producing a current, which can subsequently be amplified. Figure 17 is a schematic diagram of such a detector. The detector is usually in the form of a thin flat plate mounted on the objective polepiece, and does not interfere with normal operation of the microscope. the detector usually has four such elements. The main



disadvantage of such a detector is its relatively slow response time and its unsuitability for rapid scan rates.

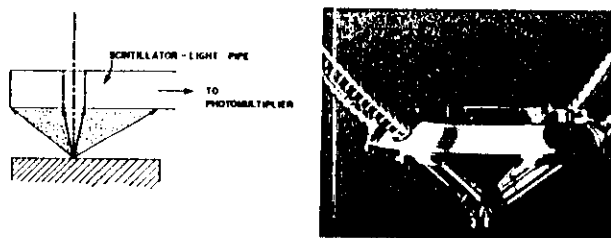


Figure 16. Scintillator backscattered detectors a) Robinson, b) multiple

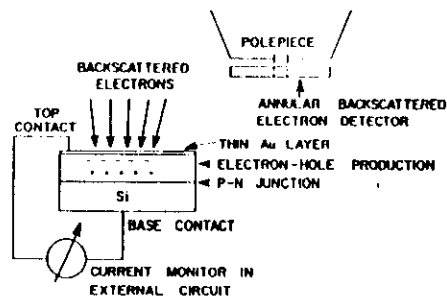


Figure 17. Solid state backscattered electron detector.

## 7.2 Compositional images

The signal from the specimen is capable of yielding information not only about the surface topography, but also the composition.

The secondary electron coefficient does not depend very much on the composition of the sample, although it may be sensitive to the surface condition and electronic structure of the material. However, the backscattered coefficient ( $\eta$ ) varies monotonically with atomic number as shown in figure 18.

It is almost independent of accelerating voltage, and Heinrich has shown that it may be expressed analytically as :-

$$\eta = -0.254 + 0.016Z - 1.86 \times 10^{-4}Z^2 + 8.3 \times 10^{-7}Z^3 \quad 21$$

The backscattered coefficient from a compound or phase containing several elements may generally be obtained from equation 21 by using a rule of mixtures based on weight fraction, although there may be a small dependence of on density.

The magnitude of the compositional or atomic number contrast from two phases of backscattered coefficients  $\eta_1$  and  $\eta_2$ , where  $\eta_1 > \eta_2$  is readily calculated using equation 13 as :-

$$C = \frac{\eta_1 - \eta_2}{\eta_1} \quad 22$$

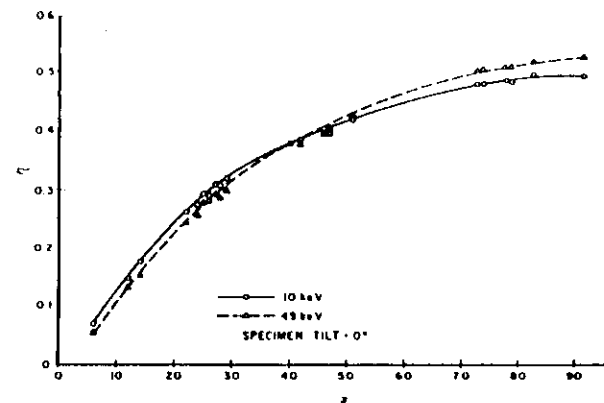


Figure 18 Variation of backscattered coefficient with atomic number.

Table 1 gives some examples of atomic number contrast calculated from equation 22

TABLE 1 ATOMIC NUMBER CONTRAST

Phase 1	Z1	Phase 2	Z2	1	2	Contrast %	Resolution degradation (nm)
Al	13	Mg	12	0.153	0.141	7.6	19
Al	13	Cu	29	0.153	0.304	49.4	5
Al	13	Pt	78	0.153	0.485	68.4	4
Cu	29	Zn	30	0.304	0.310	2.3	47
brass 29.35		brass 29.45		0.305	0.306	0.2	264

It may be seen from Table 1 that the contrast from adjacent elements is quite small, typically 1-5%, and that contrast from different phases in an alloy may be even less. Therefore, in many systems of interest, this is a relatively weak form of contrast compared to topographic contrast which may approach 100%. Specimens for compositional imaging should therefore preferably be polished flat. For compositional imaging, the solid angle of the detector should be as large as possible, and therefore short working distances and large active detector areas, either scintillator or solid state, are desirable.

Although we may be able to detect two phases in a specimen, we may not be able to do so with very good spatial resolution, because, as we saw in section 5, the ultimate resolution of the instrument is dependent on the contrast. Having calculated the atomic number contrast from equation 22, we can insert this value into equations 13 and 20, and hence calculate the spatial resolution of the two phases. This figure, shown in the last column of table 1, should be considered as a degradation of the resolution, beyond that of 0.1 μm due to the limitations of the sampling volume. It is very noticeable, that for phases with similar atomic numbers the resolution may be very poor.

It is possible to obtain quantitative compositional information by measuring the intensity of the backscattered signal from the phase of interest, comparing

it with a standard element, and then using figure 18 to obtain the atomic number of the phase. Although this technique is potentially valuable for phases of low atomic number, as these are not easily determined using x-rays, great care must be taken to exclude other forms of contrast, such as topographic or crystallographic effects.

### 7.3 Crystallographic information from the SEM

Similar electron beam interactions to those used in the TEM enable us to obtain crystallographic information in the SEM.

#### Channelling contrast

The backscattered electron coefficient is dependent on the orientation of a crystal with respect to the incident beam. This effect, known as **electron channelling**, arises from the effects of diffraction on the depth of penetration of the primary beam into the specimen. The further the primary beam penetrates, the less likely are backscattered electrons to escape, and therefore the lower is the backscattered electron coefficient. Channelling contrast is generally much weaker than atomic number contrast, and may only be satisfactorily obtained with a good backscattered electron detector, a carefully prepared specimen which must not have a deformed surface layer such as is introduced by mechanical polishing, and optimisation of the microscope operating conditions. In particular, the electron beam must be reasonably parallel, and have a large current.

#### Diffraction patterns

Although we cannot obtain diffraction spot patterns in the SEM, as we can in the TEM, we can make use of electron channelling from diffraction patterns. As discussed above, the backscattered electron coefficient from a crystalline specimen is dependent on crystallographic orientation. Therefore if we rock the electron beam over a point on the specimen surface, as shown in figure 19, the backscattered electron yield will vary. This signal may be used to modulate the intensity of the c.r.t spot whose position is a distance from the centre of the screen which is proportional to the rocking angle.

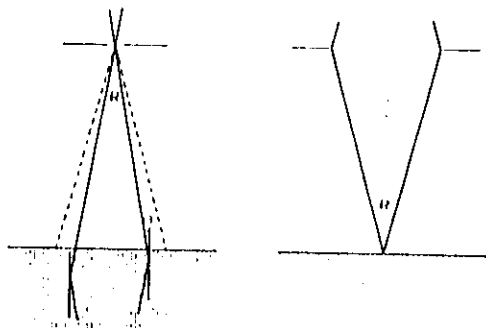


Figure 19. Method of obtaining selected area channelling patterns.

The resulting pattern is known as a **selected area channelling pattern (SACP)**. Although their methods of formation are not identical, the SACP is

geometrically similar to a TEM Kikuchi line pattern, and it is analysed in the same manner.

Although the beam in figure 19 is shown as being rocked over a point on the specimen, the electron beam is tilted at an angle of up to from the optic axis during this process. Therefore, the beam suffers spherical aberration in proportion to the cube of this angle according to equation 9. For a typical SEM lens of  $C_s = 20\text{mm}$ , and a rocking angle  $\alpha$  of 10 degrees, this will mean that the beam actually wanders over the specimen by  $\sim 13\text{ }\mu\text{m}$  during a raster, and this therefore limits the spatial resolution of this technique. Note that the objective lenses of hybrid TEM/SEM instruments, have much smaller values of  $C_s$ , and in these instruments, a spatial resolution of  $\sim 1\text{ }\mu\text{m}$  may be achieved.

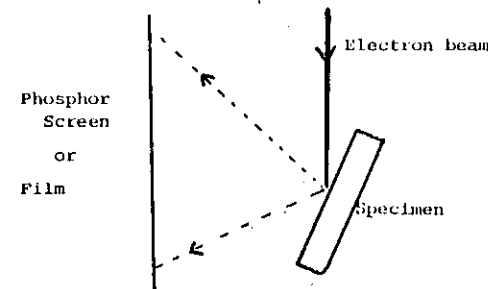


Figure 20. Method of obtaining Electron backscatter patterns.

An alternative method of obtaining a similar diffraction pattern is to keep the beam stationary on the specimen, and to collect the backscattered electrons on a film or phosphor viewing screen as shown in figure 20. In order to obtain adequate contrast in such an **electron backscatter pattern**, the specimen must be tilted through a large angle ( $\sim 70$  degrees). Although this technique requires modification to a standard SEM for the detection system, it does have a substantially better spatial resolution ( $\sim 0.1\text{ }\mu\text{m}$ ), and produces patterns with a much larger angle, and with more detail. Both types of diffraction pattern are frequently used in conjunction with channelling contrast images, to determine the crystallographic orientation of features such as grains or subgrains in a specimen.

## 8. THE USE OF OTHER SIGNALS IN THE SEM

### 8.1 The charge collection mode

Every incident electron generates hundreds or even thousands of "electron-hole pairs" when it knocks electrons from the outer shells of the atoms of the specimen, giving rise to a free electron and a "hole" in the outer shell. Normally the vast majority of these pairs recombine within about  $10^{-12}$  seconds - in other words the electrons jump back into their places in the shells extremely quickly. However, if the specimen is a semiconductor, and a voltage is applied across it, then the electrons and holes will be dragged apart before they can recombine, and a current will flow between the electrodes. Alternatively, recombination of the carriers may be prevented by an internal field, such as that from a p-n junction. We can, using suitable equipment measure either the current generated in the specimen, in which case we obtain an "EBIC", (electron beam induced current) signal, or we can measure the voltage induced by the beam - "EBIV" (electron beam induced voltage). Using either of these signals we can display an image which will represent the variation of the semiconductor properties across the specimen. The current

flowing from each point will depend on the conductivity of the specimen at that point, the lifetime of electrons and holes, and their mobility (the drift speed under unit potential gradient).

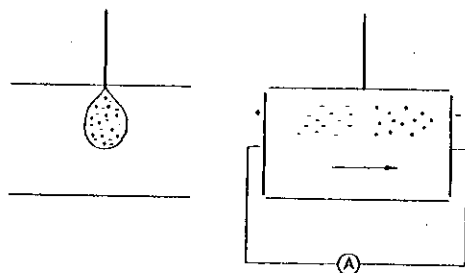


Figure 21. Charge collection current mode.

### 8.2 Cathodoluminescence

Many materials emit light under electron bombardment, and if this is detected, we can display an image in the **cathodoluminescent mode**. We have already encountered this effect in the phosphor used on the viewing screens of the transmission electron microscope and c.r.t tube of the SEM, and in the scintillator electron detectors used in the SEM. Cathodoluminescence varies in colour and intensity as a function of the composition of many minerals, and in semiconductors such as Gallium Arsenide. Consequently this mode of imaging is of particular importance in these fields of application. Cathodoluminescence is also observed in polymeric or biological material, although its use is less well developed in these areas.

As light detectors are usually also sensitive to electron, CL detectors have to be designed to remove the electrons.

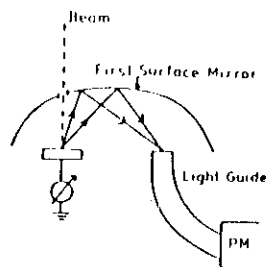


Figure 22. Ellipsoidal mirror for CL detection.

CL appears as a band of wavelengths with a peak at a photon energy which is related to the energy gap between the filled valence band and empty conduction band of semiconducting and insulating materials. Any alteration in the energy gap due to local changes of temperature, crystal structure or impurity level will lead to a change in emission. At temperatures at or near liquid helium temperature, the CL emission bands generally become more intense and much sharper, and the band may be resolved into a line spectrum. Analysis of such a spectrum enables very low levels of impurity ( $<0.01\text{ppm}$ ) to be identified. Note that this is several orders of magnitude more sensitive than x-ray analysis. CL is being increasingly being used to study the nature and distribution of

defects in opto-electronic materials and devices such as GaAs, and is capable of providing detailed and important information about the electronic effects of these defects. However, interpretation of CL data is difficult, and requires a good understanding of the solid-state physics of the material.

### 8.3 Magnetic contrast

Magnetic materials have their own contrast effects, because the magnetic field of a specimen will interact with the secondary and backscattered electrons. The SLM may therefore be used to determine the magnetic domain structure of the material.

### 8.4 Specimen current

The **specimen current**, which is the current flowing to earth from the specimen is sometimes used as a signal. As the specimen current is related to the number of electrons impinging on the specimen, less the number emitted as backscattered or secondary electrons, it gives a signal which is the inverse of the total electron emission. However, the advent of more efficient electron detectors has meant that this signal is now no longer of great interest for imaging, although it is usually monitored, because it enables the beam current to be measured.

### 8.5 STEM

The **transmitted electron beam** from a thin sample is, of course the basis for transmission microscopy. Using a scintillator detector below the specimen in an SEM, or, alternatively, using a scanning system with a TEM, results in a **scanning transmission electron microscope or STEM**.

The resultant image from a STEM is similar to that from the same specimen in a TEM. The advantage of using STEM is that the image data is produced in serial form, and may therefore be readily processed. Although this has found some application with low contrast materials, and those which degrade rapidly under the electron beam, this technique, when used in conjunction with a standard TEM or SEM is not widely used. However, purpose built, or dedicated scanning transmission microscopes, with ultra high vacuum systems, and field emission electron guns are powerful analytical instruments.

### 8.6 Scanning electron acoustic microscopy

SEAM is a new technique. Acoustic waves are generated in the sample by rapidly modulating the SEM beam. reflection and scattering occurs from both surface and subsurface features in the specimen.

## 9. IMAGE ACQUISITION, PROCESSING AND STORAGE

One of the major differences between the TEM and the SEM, is that in the latter, we acquire the data gradually, pixel by pixel, and line by line, whereas in the former, all the picture elements are built up together. Using computer terminology, we say that the SEM has **serial** data collection, and the TEM has **parallel** data collection.

The imaging data for the SEM comes as a varying electrical signal from the detector, and it is therefore easy to modify this signal with an amplifier.

### 9.1 On-line processing

The simplest on-line processing involves the adjustment of image **brightness** and **contrast** using a linear amplifier. Controls for this will be found on all microscopes.

The amplifier allows the operator to "back-off" the DC part of the signal, and to expand the useful AC part.

In most circumstances this is all that is required to produce a good image on the c.r.t., but some microscopes offer other signal processing options which may be of use in certain circumstances.

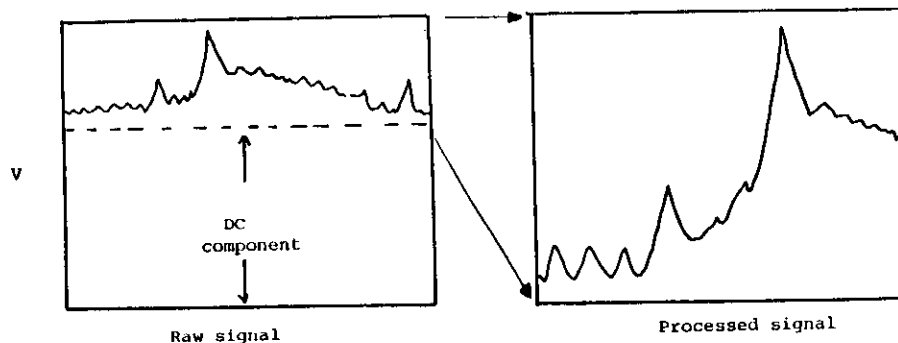


Figure 23. Optimising a signal using contrast and brightness controls.

For example, if we wanted to emphasise the dark features X in the image, we could use nonlinear amplification. Instead of the amplifier output being proportional to the input, as it would be in a linear amplifier, we might arrange for  $V_{out}$  to be proportional to the square root of  $V_{in}$ . This would then amplify the dark features more than the light ones, as shown in figure 25. This is called **Gamma control**, after the term used to specify the grey level response of photographic film.

Another type of processing sometimes used is **signal differentiation**, in which the output voltage of the amplifier is proportional to slope of the voltage/time curve. This emphasises regions where the signal changes rapidly, but flattens the contrast from a gradually changing background.

It is also sometimes useful to add signals from different detectors or subtract them from each other.

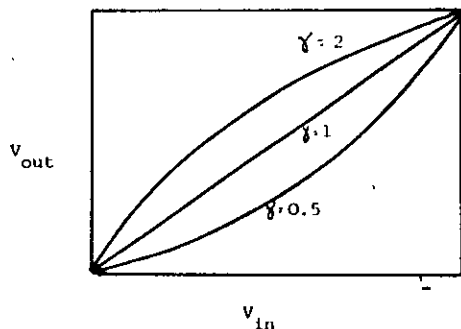


Figure 24. Gamma processing.

It is easy to manipulate the incoming signals in a variety of ways, and to produce some very interesting results. However, the interpretation of the images may not be straightforward, and any but the simpler methods of signal processing should be used with caution.

## 9.2 Scan rates and data storage

The microscope operator will need not only to view the scanned image so as to identify features of interest, focus and optimise the image, but also to obtain a permanent record of the chosen image. These two requirements often conflict.

We saw in section 5, that in order to produce a good quality, noise free image from a given specimen, a minimum beam current is required, and that this is inversely proportional to the time for a frame scan (F). Figure 13 shows how the minimum useable probe size, which is approximately equivalent to the spatial resolution for secondary electrons, varies with specimen contrast and frame scan time.

The best quality images are needed for photographic recording, which is carried out with a camera focussed on a high resolution c.r.t. The scan rate is slowed right down so that one frame takes typically 50-100 seconds, while the camera shutter is open.

If the scan is carried out at rate of 50 frames per second then the display appears simply as a television image. This is very convenient if the operator wants to move the specimen, focus the image, or simply to see what the specimen looks like. Also under these conditions, the microscope can be interfaced to a TV monitor or videorecorder. However, as may be seen from figure 13, the price that must be paid for such a fast scan rate is a dramatic loss of resolution. For example, considering a specimen with a contrast level of 50%, we see that although we might achieve a resolution of ~5nm with a 100 second scan time recorded on photographic film, with a TV scan rate, the resolution drops to 100nm. If we further assume that a TV system has a resolution of 500 x 500 pixels, then, using the arguments of section 5, it can be seen that the maximum useful magnification in these circumstances will be x3000.

If it is necessary to work at higher magnifications, so as for example to focus an image for photographic recording, then operator must compromise, and work with a slower scan rate, perhaps one or two frames per second.

This problem is even more acute when a detector with a slow response time, such as a solid state backscattered detector is used. In this case, fast scan rates cannot be used at any magnification.

## 9.3 Digital image storage

Some of the problems and inconvenience associated with slow scan rates can be overcome by the use of **framestores**, which are increasingly being used in conjunction with scanning electron microscopes. The operation of the framestore is most easily explained by referring back to figure 2b. In normal operation, as the beam scans the specimen, the corresponding pixels on the c.r.t are momentarily illuminated. However, it is possible to transfer this transient reading to a computer memory, and therefore after a complete scan, we will have a digitally recorded, or digitized the image. The computer will usually require as many data storage locations or bytes of memory, as pixels, and each of these will be able to store the intensity as a number between 0 and 255 for an 8 bit computer, or 0 and 65535 for a 16 bit computer. We saw earlier that a high resolution c.r.t has a resolution equivalent to 1000 x 1000 pixels, and an equivalent framestore would be one of 1024 x 1024 bytes, or one megabyte. The framestore is designed to transfer its data rapidly to a monitor screen (VDU), so that the stored pixel data is represented as a point of the appropriate intensity on the VDU, and therefore the frame which we have scanned once, is now displayed permanently on a screen whilst the image on the c.r.t. disappears almost immediately.

This has an obvious advantage for slow scan rates, because we can use a very slow scan rate which would be very difficult to see on the c.r.t., and then view it on the VDU. This is also of application to beam sensitive materials, as processing of the image may be carried out after acquisition, as discussed below, rather than whilst the specimen is being viewed in the microscope.

However, framestores are equally useful at rapid scan rates because they can be used for **frame averaging**. In this mode, the data in the frame store is updated to an average value after every frame, and therefore the noise on the VDU continually decreases as the number of frames increases. In terms of image quality, a frame store which has run for 500 frames at a scan frequency of 50

per second is equivalent to a single scan of 10 second duration, but it has the advantages that the operator can see an image all the time, instead of waiting for a film to be processed. The data in a framestore may be stored in the same way as any other computer data, and it thus has the permanence of a film.

#### 9.4 Processing stored images.

One of the advantages of a digitized image over a photograph is that the data may be manipulated in a wide variety of ways after it has been recorded.

All the basic on-line processing options such as contrast and brightness optimisation, gamma control and differentiation, which were discussed above, can be carried out on a digitised image. In addition, **grey level contouring**, in which the number of grey levels is reduced, so that all regions of similar contrast appear with the same grey level, is readily done. This is particularly useful for identifying phases in a compositional image.

With a digitized image, a whole variety of options are open for obtaining further quantitative data from it. These include measurement of phase volume fractions and the sizes and shapes of particles, diffraction pattern analysis, image comparison, and pattern recognition.

This science of **image analysis** is a rapidly developing and exciting field, but as the techniques are not specific to electron microscope images, further discussion here is not warranted.

#### 9.5 The Digital SEM

We have discussed the advantage of adding a framestore to the microscope in order to collect and process data. There are advantages to be gained from going further along these lines. Instead of just collecting the signal at appropriate intervals during the scan, we could actually control the scan with a computer so that instead of moving the beam in a scan raster as shown in figure 2a, we moved the beam directly to the required pixel points of figure 2b, and allowed it to dwell on each point for a predetermined time. We would, at the same time, collect not only one signal, but all the available ones, including perhaps several different types of x-ray signal.

This type of digital control of the microscope has been pioneered by the manufacturers of x-ray analytical equipment for digital x-ray mapping. However, before long, it is likely that digital scanning will be an integral part of all scanning electron microscopes

## INTRODUCTION

### To energy-dispersive X-ray microanalysis

The development, over the last 15 years, of the solid state energy resolving x-ray spectrometer has revolutionized x-ray microanalysis. Due to its speed and simplicity the energy-dispersive spectrometer, (EDS), is now the most common x-ray measurement instrument to be found on an electron microscope. With EDS all elements present in the specimen at concentrations of greater than 10 weight% can be identified in less than 10 seconds, minor constituents down to 0.5 wt% can be analysed in 100 seconds. As well as identifying which elements are present in the sample EDS can also tell how much and where the elements are distributed.

Understanding and using an ED system brings one into contact with several areas of interest: the basic physics of x-ray production, semiconductor theory with regards to the detector, the electronics of signal amplification and measurement in the processor, and computer studies involved in handling the data. The aim of these notes is to give a brief background knowledge on each topic, and more importantly to offer some basic guidelines on how to use an ED system.

When an electron probe interacts with a material x-rays are formed. The volume over which the incoming electrons penetrate is known as the **interaction volume**. The shape of this interaction volume is shown in Figure 1.

The actual dimensions of the volume are dependent on:-

- \* Accelerating voltage, (ie the energy of the electrons)
- and
- \* Density of the material, (or mean atomic number)

At high kV the electrons have a greater energy and a greater penetration power. For example, the depth in material of density of 3 at 30 kV is approx 3 microns, but at 10 kV the penetration is approximately 1 micron. The density of the material also affects the penetration depth. Both these effects are shown schematically in Figure 2.

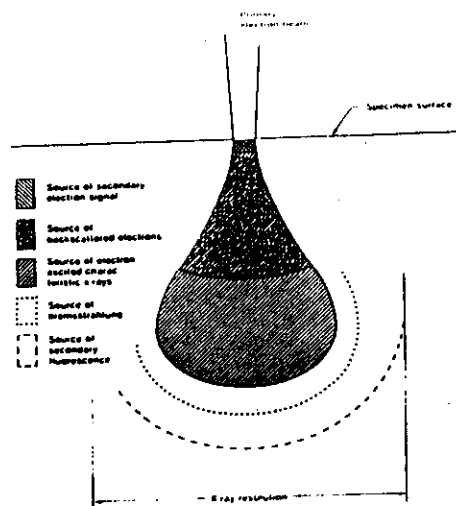


Figure 1: Interaction Volume.

In low density materials there are relatively few electrons in the atoms. Electron scattering is therefore reduced and the electrons can travel further into the material before losing all their energy from collisions with atoms. Higher density (atomic number) materials have more electrons per unit volume and therefore incoming electrons lose their energy from collisions over a much smaller depth. For example at 30 kV, a material of density 3, penetrates to a depth of 3 microns, a material with density of 10 at the same kV will have a penetration depth of approximately 0.8 microns.

X-rays generated over the whole of the electron interaction volume can find their way into the x-ray detector. This has an important consequence with respect to the "width" of the region in the sample that is being analysed, i.e. the SPATIAL RESOLUTION. This X-ray spatial resolution is always larger, and essentially independent of the diameter of the electron beam. This is illustrated in Figure 1. As an example, at 20kV the x-ray spatial resolution is of the order of 1-2  $\mu\text{m}$ , irrespective of image resolution.

X-ray can find its way into the x-ray detector. This has an important consequence with respect to the "width" of the region in the sample that is being analysed, i.e. the SPATIAL RESOLUTION. This X-ray spatial resolution is always larger, and essentially independent of the diameter of the electron beam. This is illustrated in Figure 1. As an example, at 20kV the x-ray spatial resolution is of the order of 1-2  $\mu\text{m}$ , irrespective of image resolution.

The table in Appendix 1 gives a rough idea of different penetration depths for varying operating voltages and densities.

The penetration depth

The table in Appendix 1 gives a rough idea of different penetration depths for varying operating voltages and densities.

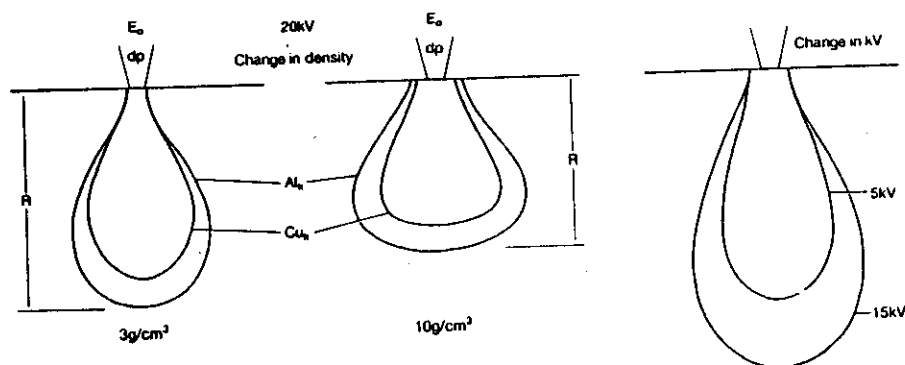


Figure 2: Variation of the X-ray interaction Volume with Density and Operating Voltage.

## X-RAY GENERATION

When electrons interact with a material, X-rays are produced. The energy range of the X-rays is from zero up to the energy of the incoming electrons. Two types of X-rays are produced, background radiation, and characteristic radiation. Each type of radiation is produced by a different type of interaction.

### Background Radiation

Background radiation, (also known as continuum, bremsstrahlung and white radiation), is generated as the incoming electrons penetrate the material and slow down in the magnetic field associated with the atoms. Background X-rays cover the whole energy range from zero up to the energy of the incoming electrons. They provide no information on which specific atoms are present, only the mean atomic number of the specimen. In simple terms, an X-ray is produced when the incoming electron collides with an atom and loses some of its energy in the collision, (thereby "slowing down"). The energy of the X-ray depends on the amount of energy lost by the electron in the collision which in turn depends on the collision angle. For example in a direct collision the electron may lose all its energy and the resultant X-ray would have an energy equal to that of the incoming electron. This always represents the maximum energy an X-ray can have. The energy distribution of X-rays depends on the kV and is shown schematically in Figure 3.

This figure shows the X-ray distributions generated when a piece of Co is irradiated with electrons of increasing energy. Curve A represents 3 kV electrons. The curve is smooth with a cut-off at 3 keV. Curve B represents 5 kV electrons, again the curve is smooth but this time has a cut-off at 5 keV. When 10 kV electrons are used a peak appears on the curve at an energy of 6.9 keV. An X-ray of this energy is generated when an incoming electron interacts with the inner shell of a Co atom, and is known as Characteristic radiation.

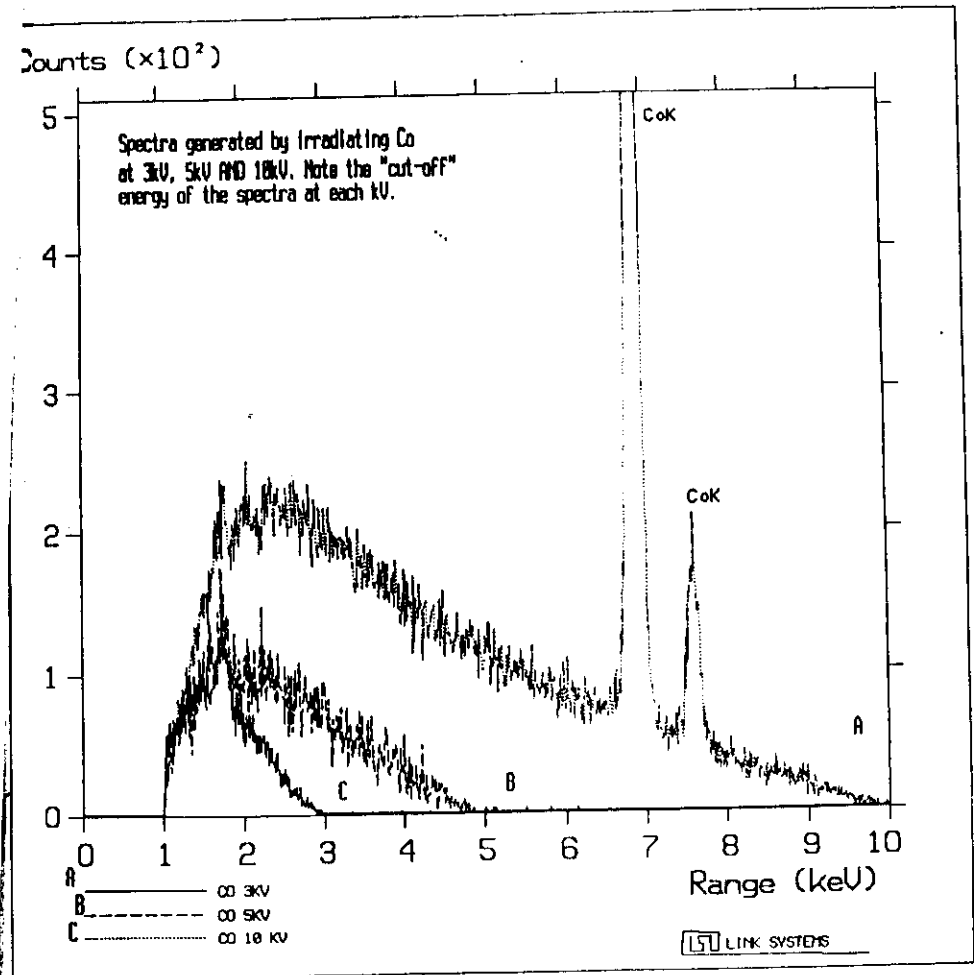


Figure 3: Variation of X-ray Production with kV

### Characteristic X-ray Production

An incoming electron can interact with the inner shell electrons of an atom, with the result that an electron is ejected from its shell, as illustrated in Figure 4. The atom is left in an ionized (and unstable) position.

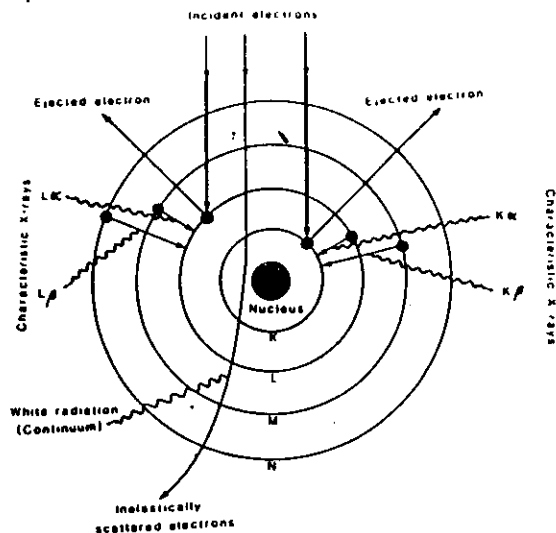


Figure 4: Production of Characteristic X-rays.

The potential energy of the atom is reduced if an electron from one of the higher energy outer shells, falls to occupy the vacant position in the lower energy inner shell. The reduction in potential energy is released in the form of an x-ray. The energy of the x-ray produced is determined by the difference in energy between the sharply defined quantum energy levels in the atom. Because energy levels in an atom are unique to each atomic number, the x-ray produced is characteristic of the atom from which it was emitted, hence x-rays produced from interactions with the inner shells of the atom are known as characteristic x-rays. It is this type of radiation that is most useful in x-ray analysis.

When an electron is ejected from the K shell, the radiation is known as a K line, likewise ejection from the L or M shell produces L and M lines respectively. The actual energy of the

result  
possib  
names

resultant X-ray depends on exactly which transition, of the many possible transitions has occurred. A broad outline of the different names given to the different transitions is given in Figure 5.

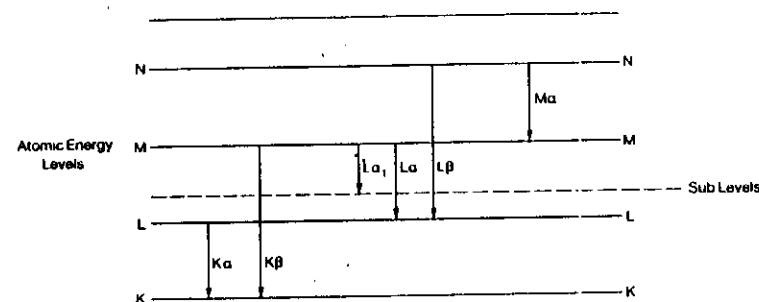


Figure 5. Production of Characteristic X-rays from different Energy Levels from within the Atom.

If t  
from  
than  
M st  
is :  
be :  
Thu  
she  
she  
she  
no  
she  
hea  
hav  
tha  
spe

If the vacant K shell position is occupied by an electron falling from the L shell (Kα) the X-ray will obviously have a lower energy than if the position was occupied by an electron falling from the M shell (Kβ), where the energy DIFFERENCE is larger. As each shell is split into sub-levels, the number of possible transitions can be large, especially as the atomic number of the atom increases. Thus for Carbon, (Z=6), with two K shell electrons, and four L shell electrons, only Kα x-rays can be generated. Although the L shell electrons in carbon can be ejected in a collision, there are no M shell electrons to fill the vacancy. Sodium (Z=11) has one M shell electron, so that both Kα and Kβ x-rays can be emitted. A heavy element like lead, with its complicated shell structure will have a very extensive family of lines. Many of the transitions that occur cannot be resolved by an Energy Dispersive spectrometer.

As  
ba  
el  
sh  
Be  
th  
ha  
x-

As shown in Figure 3, when irradiating Mn, below a certain kV only background radiation is produced. In this case the incoming electrons do not have enough energy to remove an electron from its shell. Because the energy of each shell and subshell is sharply defined, the minimum energy necessary to remove an electron from a shell has a specific value, the so-called critical ionization energy (or x-ray absorption energy). Each shell and sub-shell requires a



different critical ionization energy. As an example Table 1 shows the critical excitation energies for the L, L, and M shells and sub-shells of Platinum (Z=78).

Critical Ionization Energies for Pt

SHELL	ENERGY (keV)
K	78.39
L1	13.88
L2	13.27
L3	11.56
M1	3.396
M2	3.026
M3	2.645
M4	2.202
M5	2.122

Within a particular x-ray series, the line which will be most efficiently excited is always dependent on the accelerating voltage of the microscope. For example, when analysing Pt at 20 kV, the major line in the spectrum is the M line at 3.9 keV. The K line will not be present at all. An accelerating voltage of at least 80 kV would be needed if a tightly bound electron from the K shell is to be ejected. In fact, to efficiently excite any x-ray line the accelerating voltage used should be at least 2.5x higher than the energy of the x-ray line. Consequently, we can see from the table above, that the Pt L line will not be efficiently excited at accelerating voltages of less than 30 kV. The laws of probability dictate that if the incoming electron energy exceeds the critical excitation energy, then that transition will occur. This fact is a useful aid in identifying elements in the spectrum, (see section on qualitative analysis).

#### Efficiency of X-ray Production

The efficiency of x-ray production, even at constant operating voltage varies with atomic number. Ultimately the probability of x-ray emission during electron radiation is equal to the product

of two probabilities, (1) inner-shell ionization and (2) x-ray production resulting from radiative transitions.

#### The ionization cross-section (Q).

The probability that an atom will be ionized by an incoming electron of a particular voltage is given by the ionization cross-section. This parameter can be calculated and is a function of the energy of the incident electron and the critical ionization energy of the particular shell of the element concerned.

The ionization cross-section (Q).

The probability that an atom will be ionized by an incoming electron of a particular voltage is given by the ionization cross-section. This parameter can be calculated and is a function of the energy of the incident electron and the critical ionization energy of the particular shell of the element concerned.

#### The fluorescence yield (W).

Only some inner-shell ionizations lead to the release of an x-ray. The energy released during some transitions may be imparted to eject an electron from an outer orbit, this is an Auger electron. The x-ray fluorescence yield is the fraction of ionizations that lead to x-ray emission. The value of W is a function of atomic number and approaches zero for:- Be K shell, Ca L shell, and La M shell ionizations. These elements represent the limits of x-ray production for their respective series. The relationship between fluorescence yield and atomic number is shown in Figure 6.

Only some inner-shell ionizations lead to the release of an x-ray. The energy released during some transitions may be imparted to eject an electron from an outer orbit, this is an Auger electron. The x-ray fluorescence yield is the fraction of ionizations that lead to x-ray emission. The value of W is a function of atomic number and approaches zero for:- Be K shell, Ca L shell, and La M shell ionizations. These elements represent the limits of x-ray production for their respective series. The relationship between fluorescence yield and atomic number is shown in Figure 6.

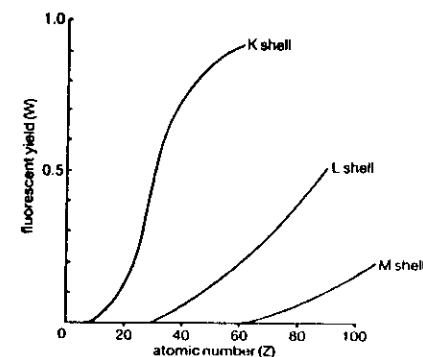


Figure 6: Relationship between fluorescence yield (W) and Atomic Number (Z).

## HANDY FACTS:

\* The units of energy in the spectrum are electron volts. This derives from the fact that when an electron travels through a potential of 1 volt, it acquires an energy of 1 electron-volt (eV).

\* The maximum X-ray energy generated is equal to the energy of the incoming electron. Therefore the cut-off energy of the X-ray spectrum shows what the operating voltage was. This is useful to detect specimen charging in the microscope. If the specimen is charging then the effective kV is reduced by the amount of charge present on the specimen, and can be measured by looking at the cut-off energy. For example if a material is examined with 20 kV electrons and the x-ray spectrum finishes at 15 keV, then the specimen is charging by 5 kV. This means the "effective" kV is only 15 and therefore the x-ray generation efficiency will be different from that at 20 kV, particularly for the higher energy lines. This has important consequences in quantitative analysis.

\* Critical excitation voltage is useful in qualitative analysis. If the operating voltage is less than the energy at which a particular shell is ionized we will not see a line for that shell in the spectrum. For example when identifying Pt, we may look for the M line at 2 keV, and the L lines at 9 keV. However the operating voltage is less than 10 kV Pt L lines will not be excited.

\* The x-ray interaction volume will always be slightly smaller than the electron interaction volume because on the outer edges of the electron range electrons do not have enough energy to produce x-rays, especially x-rays with high critical ionization energies.

\* Irrespective of image resolution, in a bulk sample, the x-ray spatial resolution is ALWAYS of the order of 1-2 microns.

## The ENERGY DISPERSIVE SYSTEM

The ED system can be broken down into 4 basic units. As shown in Figure 7 these comprise devices to detect the x-rays, measure their energy, display the data, and a computer to carry out any further processing on the data.

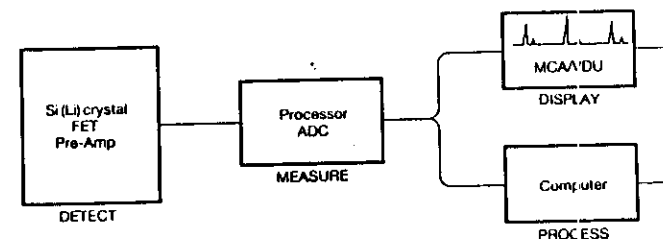


Figure 7. Block Diagram of an Energy Dispersive System.

To summarise the operations of an ED system:-

1. X-rays pass through a thin Beryllium window into a cooled, reverse bias, Lithium drifted Silicon crystal. The crystal converts the x-ray energy into a pulse of electrical charge. An individual x-ray liberates around  $10^{-14}$  coulombs of charge.
2. The charge pulse is converted into a voltage pulse at the PRE-AMP. This charge to voltage conversion actually takes place at the FET, (Field Effect Transistor). The FET also acts as the first stage amplification, and in combination with other amplifiers in the pre-amp raises the signal to a high enough level to be passed along cables to the pulse processor.
3. Once the signal has been passed from the detector into the PROCESSOR, it is further amplified prior to the energy of the pulse being measured.
4. The amplified voltage is an analogue signal. It is converted to a digital signal for measurement and display. This step is

carried out by the Analogue to Digital Converter (ADC) and the digital signal is put into a Multi-Channel Analyser (MCA). It is the contents of this MCA that we view in the spectrum on the video monitor.

### The Detector

The Si(Li) x-ray detector uses the principle of the "photoelectric effect". X-rays entering the crystal cause the movement of electrons from the valence band into the conduction band, thus generating a certain number of electron/hole pairs. The basis of an ED system is that the number of electron hole pairs produced is directly proportional to the energy of the incoming x-ray.

The detector is the most sensitive part of the whole system and consists of 3 units; the crystal, the FET and pre-amp, and a cryostat to cool the crystal and FET. A cross section of the crystal and FET is shown in Figure 8.

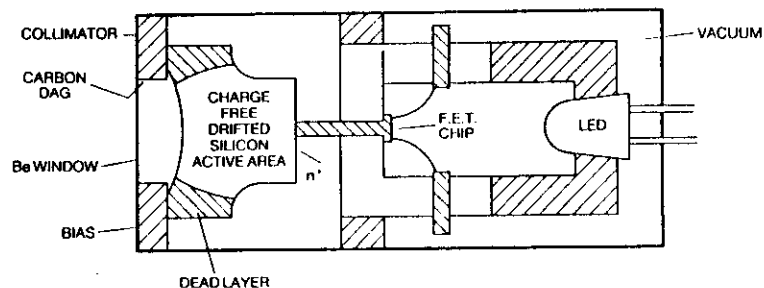


Figure 8. Schematic of the Crystal and FET.

### The Crystal

The crystal is a p type extrinsic semiconductor. The manufacturing process involves drifting high purity Silicon with a minute quantity of Indium to give a material with an excess of "holes", (i.e. p type). This is then further drifted with Lithium to "soak up" the holes. Leakage current, (transitions from valence to conduction band induced by thermal activity), is lower in p type semiconductors than in n type. Minimizing leakage current is an important step in producing a high resolution detector.

When an x-ray enters the crystal a specific number of electron hole pairs are produced. The formation of an electron hole pair requires approximately 3.8 eV, the number of pairs formed, (and thus the magnitude of the charge liberated) is directly proportional to the energy of the entering x-ray. A bias of approximately 500 V is applied across the crystal which acts to pull the negative electrons and positive holes apart, producing the charge and also preventing recombination.

The magnitude of the charge involved is exceptionally small, e.g. a 5 keV x-ray photon would produce a total of 1300 electrons, (and holes), which is equivalent to a charge of  $2 \times 10^{-14} \text{C}$ .

For accurate amplification and measurement it is necessary to convert that charge pulse into a voltage pulse. This conversion occurs at the FET.

### The FET

An FET converts changes in charge to larger changes in voltage. To understand how an FET works we can use a simple analogy with water flowing through a rubber tube. The tube has a piece of string tied at the centre. This is shown schematically in Figure 9.

When the string is loose, water flows through the tube unrestricted. If pressure is applied to the string to tighten it the diameter of the tube decreases and the water flow will decrease by an amount proportional to the pressure applied to the string. If the pressure is increased on the string there will be a corresponding decrease in the flow of water. Depending on the flexibility of the tube and the flow of water, a small pressure on the string can result in a large change in the flow of water, i.e. signal amplification occurs.

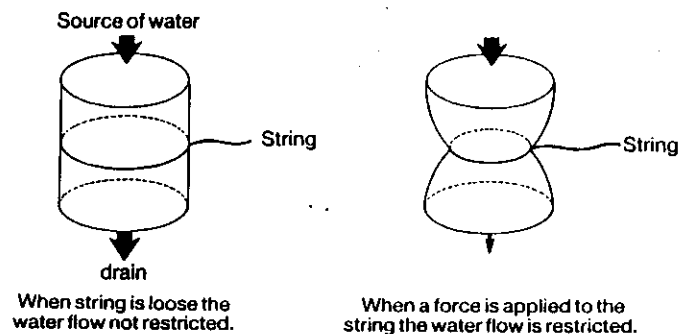


Figure 9: Schematic of an FET, analogy with water flow.

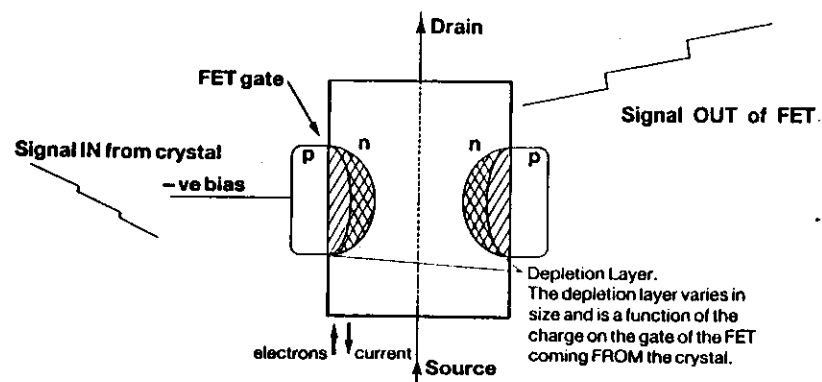


Figure 10: Schematic of an FET.

In the real situation, electrons flow through a passage in a piece of silicon. The "string" around the centre is a depletion layer formed at a p-n junction, and the pressure on the string is provided by the signal coming from the crystal. This is shown schematically in Figure 10.

A burst of charge from the crystal, (liberated by an incoming x-ray), causes a **depletion layer** to be formed in the tube. This restricts the flow of electrons. The signal going into and coming out of the FET is shown in Figure 10. If an exceptionally large burst of charge is liberated from the crystal, e.g. from a high energy electron, the subsequent depletion layer formed can block completely the flow of electrons. If this happens the dead-time goes to 100%, and it may take several hours for the depletion layer to die away.

#### Minimizing Noise

The charge generated at the crystal is extremely small and steps must be taken to ensure that the pulse is not swamped by noise. Two measures of interest used in the detector to keep noise to a minimum are:-

- \* Pulsed Optical Feedback
- \* Low temperatures

**Pulsed Optical Feedback:** Standard pre-amplifiers need resistive feedback in the circuitry to return the system to a condition where it can accept the next pulse. This type of feedback generates too much noise to be used in an energy dispersive detector and the method of pulsed optical feedback is used. In this case, instead of the FET resetting after each pulse, the pulse is stored, i.e. the voltage level stays constant until the next pulse arrives. The resultant output is a step function. In this way each pulse goes through to be amplified without the interference of any feedback noise. The output from the FET/Pre-amp is illustrated in Figure 11.

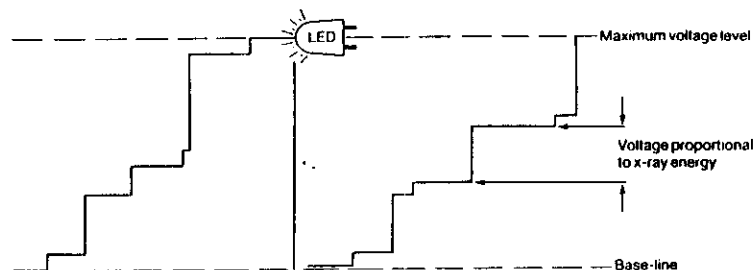


Figure 11. Schematic of Pulsed Optical Feed-back.

The FET cannot carry on indefinitely accepting pulses without being reset. Eventually a voltage is reached beyond which it cannot accept any more pulses without losing linearity and eventually becoming damaged. At this point a light emitting diode is switched on which completes a circuit and allows the FET to return back to baseline. All amplification and measurement of pulses stops while the diode is switched on. This contributes to the DEAD TIME in the system, always observed when acquiring x-ray data.

**Liquid Nitrogen Temperature:** Cooling the crystal and FET is essential to keep noise to a minimum. Low temperatures are more easily maintained by sealing the components under vacuum, which also has the advantage of reducing contamination on the crystal. Low temperatures also reduce the mobility of the Li impurity ions and helps maintain the large intrinsic, (active) region in the crystal. A cross-section of the cryostat arrangement is shown in Figure 12.

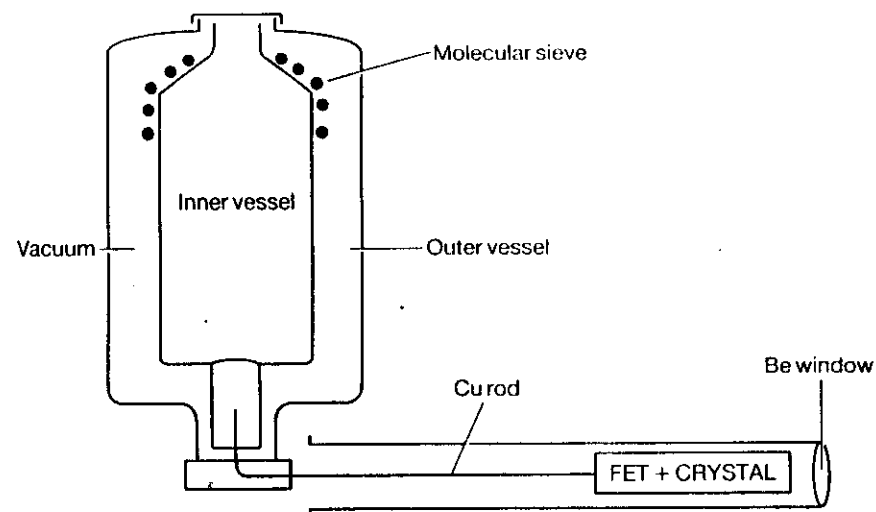


Figure 12. The Cryostat arrangement.

The liquid nitrogen is contained in a dewar which has a typical capacity of 5 litres. This requires filling every few days unless fitted with an automatic feed system. The cryostat is evacuated to better than  $10^{-4}$  torr. Outgassing is dealt with by a molecular sieve. The whole assembly must be kept under vacuum but still allow X-rays to enter. This problem is solved by using a thin Be entrance window. The window must be capable of withstanding atmospheric pressure but still be transparent to low energy x-rays. Windows of  $25\mu\text{m}$  Be give only 12% transmission at 1 keV, but 50% transmission is obtainable with  $8\mu\text{m}$  windows. Such a window will block all x-rays below energies of about 0.8 keV, limiting analysis to elements of atomic number 11 and above.

#### Detector Resolution

The natural width of an x-ray peak is about 2 eV, measuring the full width at half the maximum intensity (FWHM). The E.D. system degrades the peak by a factor of about 100. For example, for Mn K $\alpha$  a typical resolution would be 145 eV. This degradation in width of the peak occurs because, (1) there is a statistical distribution in the number of electron-hole pairs produced by a monoenergetic

x-ray and (2) an uncertainty is introduced in the amplification process. The distribution of numbers of electron-hole pairs is reasonably well described by a Gaussian distribution. The FWHM of this distribution can be calculated from the two sources of noise, according to the equation:-

$$\text{FWHM} \propto (C^2 E + N^2)^{1/2}$$

where C is a measure of the uncertainty in the number of electron-hole pairs produced, E is the energy of the incoming x-ray and N is the FWHM contribution from the electronic noise of the amplification process. The value of C is dependent on the material used in the crystal and incorporates a constant known as the Fano factor. Even if electronic noise were to be completely eliminated, the statistical uncertainty in the number of electron-hole pairs, (as represented by the Fano factor) will limit the resolution. For example the theoretical resolution for Mn is of the order of 90 eV. From the above equation we can see that the resolution decreases with the energy of the x-ray, i.e. the resolution as measured at Na will be lower than at Mn.

For a given detector the effect of noise can be minimised by correct selection of pulse shaping time constants in the main processor. However at high count rates, e.g. greater than 5000 cps, these time constants are reduced below their optimum value, causing a decrease in resolution as the count rate increases. This is one reason why x-ray analysis is not performed at high count rates.

External noise sources including vibration and electrical interference can cause loss of resolution. Susceptibility to interference is minimised by avoiding ground loops. The detector should also be isolated from the microscope and earthed only through cables. Also, all the electronic units should preferably be earthed at one point.

Resolution is also affected by the capacitance of the detector. Detectors of small area and hence small capacitance give the best performance. Therefore unless high collection efficiency is of paramount importance crystals with an area of about 10mm<sup>2</sup> are generally used.

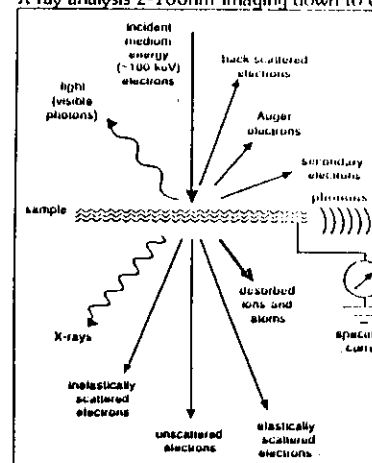
The following section deals with the most common questions asked about detectors.

## INTRODUCTION TO TEM/STEM AND X-RAY MICROANALYSIS

### WHY USE TEM/STEM

High spatial resolution microanalysis correlated with images.

X-ray analysis 2-100nm Imaging down to 0.2nm



### TEM/STEM versus MICROPROBE

ADVANTAGES	DISADVANTAGES
High spatial resolution	Sample Prep
EDS, EELS, SE, BS, BF, DF	Low Sensitivity
Diffraction, CBED, microdiffraction	Low accuracy of quantitation
Quick qualitative analysis	Yield
High vacuum	High vacuum
Low beam spreading	Beam damage

### ELECTRON SOURCE CHARACTERISTICS

#### BRIGHTNESS

$$\beta_s \propto E_0$$

Maximum current limited by lens aberrations.

#### COMPARISON OF SOURCES

	W	LaB <sub>6</sub>	FE
$\beta_s$	$3 \cdot 10^5$	$3 \cdot 10^6$	$10^9$
stability	1%	2%	1-5%
source size	50µm	1µm	5nm
energy spread	3eV	1eV	0.25eV
probe dia for 1nA	40nm	20nm	1nm

**STATISTICAL REQUIREMENTS****STATISTICAL LIMIT ON ACCURACY:**

$$95\% \text{ confidence} - 2\sigma \quad \% \text{ accuracy for } N \text{ counts} = \frac{2\sqrt{N}}{N} \cdot 100$$

$$99\% \quad " \quad 3\sigma \quad " \quad = \frac{3\sqrt{N}}{N} \cdot 100$$

$$\text{i.e. for } 2\% \text{ accuracy at } 95\% \text{ level need } N=10^4$$

$$3\% \quad N=10^6$$

$$\text{NB} \quad \text{EDS 'peak' is real only if } I_B > 3\sqrt{2I_B^b}$$

See Trebbia: Ultramicroscopy, 1988, 24, 399-408.

**MINIMUM MASS FRACTION**

$$C_B \text{ (MMF)} = \frac{3\sqrt{2I_B^b}}{I_A - I_A^b} \cdot \frac{C_A}{k_{AB}}$$

$C_A$  = Concentration of A

$k_{AB}$  = sensitivity factor

Implies need long counting times and low background

**BEAM BROADENING**

Previous section makes it tempting to work in thicker parts of the specimen to get a higher signal but beam broadening due to scattering will degrade spatial resolution.

$$b \propto \frac{Z\sqrt{t^3}}{E_0}$$

This assumes single scattering, and  $b$  = probe size containing 90% of electrons exciting specimen

(See Loreto p 175)

**b versus t examples**

t	50nm	100nm	300nm
Al	3	8	42
Cu	7.5	21.5	112
Au	17	-	-

e.g. for 4nm incident probe on 100nm Cu foil spatial resolution becomes:

$$\sqrt{4^2 + 21.5^2} = 22\text{nm}$$

Important to know foil thickness --> use EELS or CBED.

**ARTEFACTS**

Four principle sources

**Illumination System**

Hole Count - x-rays, electrons, light.

**Sample / Sample Holder**

Specimen bremsstrahlung, scattered electrons

**X-ray - Specimen Interaction**

Absorption (importance increases as separation of x ray energies increases)

Fluorescence (negligible for  $Z > 20$ , important for elements of adjacent  $Z$ )

Coherent bremsstrahlung

Beam broadening

Electron channelling

**Detector**

Escape peaks, sum peaks, dead time, incomplete charge collection, detector efficiency.

**SEM / microprobe**

Low kV means hole count very low

No electrons transmitted through specimen

Large specimen chamber

Normally zero tilt

**'IDEAL' SPECIMEN**

Crushed sample on holey carbon film on a beryllium grid.

Zero tilt and high take off angle.

Specimen fragments small therefore absorption negligible.

Specimens must be clean and minimal surface films and oxide layers.

Count rate approx 3000cps total.

Avoid strong diffraction conditions in alloys and compounds.

**CLEANING SPECIMENS**

Make final washes in very high purity solvent (e.g. Aristar grade).

Bake in air or clean vacuum to approx 100C.

Use cold stage at -70C if contamination is still a problem.





For large collection angle (i.e. ADE)

$$\sigma_{\text{elastic}} \propto \sqrt{Z^3}$$

### Phonon Scattering

Atomic bond vibration; collective lattice vibration in crystals.

Energy losses very small  $\approx 0.1\text{eV}$  but scattering distribution a broad peak centred around each

Bragg reflection  $\rightarrow$  again reduces number of inelastic electrons collected.

### Importance and Use

Measure of spectrometer performance, stability and resolution

Used in alignment

Normalization factor for absolute quantitation

### Region 2 - Low-Loss (0-100eV)

Zero Loss peak contains 80% of total signal, 0-50eV contains a further 5-10%

Low losses due to direct electrostatic interactions with atomic electrons.

Losses <15eV excitation of electrons in molecular orbitals, >15eV mostly valence shell excitations

Peak shape and positions can change dramatically as a function of valence state of metals and oxides.

Metallic conductors generally have a simple valence band structure which can be described in terms of a collective plasmon interaction.

### Plasmon Losses

Free-electron metals and alloys  $\rightarrow$  simple low loss spectrum - sharp gaussian peaks. Number and intensity related to specimen thickness, peak energy related to mean electron density in conduction band.

Free electrons behave as 'gas' in equilibrium density due to coulomb repulsion. Incident electron disturbs equilibrium  $\Rightarrow$  oscillation  $\rightarrow$  'collective excitation'.

Oscillation frequency  $\omega_p \propto \sqrt{n_e}$   $n_e$  = electron density

Energy to cause oscillation,  $E_p = \hbar\omega_p$

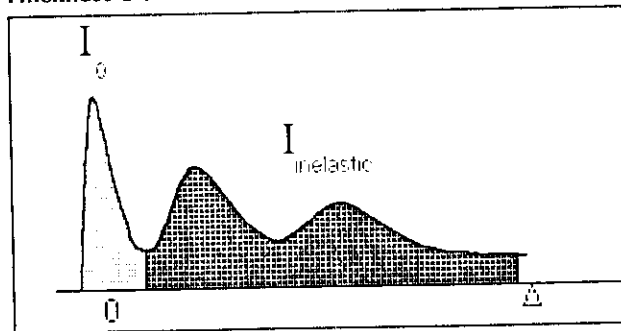
Incident electron energy loss =  $E_p$  typical values  $\omega_p \approx 10^{16}$  rad/s;  $E_p \approx 20\text{eV}$

Scattering over large angular range (5-10mrad), then rapid fall off.

Plasmon mean free path,  $L_p \approx 50-100\text{nm}$  at 100kV

Thick specimens give multiple plasmons

### Specimen Thickness Determination



$$t = L_p \ln \left[ \frac{I_0 + I_{\text{inelastic}}}{I_0} \right]$$

$t/L_p < 0.1$  surface plasmons dominate

$t/L_p > 0.5$  not linear - too thick for microanalysis

If know  $L_p \rightarrow t$  and vice versa

$t$  can be measured to  $\pm 10\%$  (in range  $t = 10-150\text{nm}$ )  
(see Egerton & Cheng, Ultramicroscopy, 21, 1987:231)

### Region 3 - Core Shell Losses

Above 50eV spectrum consists of a rapidly decaying background due to single-electron valence shell interactions with superimposed 'core loss' edges arising from inelastic interactions with inner shell electrons.

Thus to ionise an atom need to transfer a minimum amount of energy,  $E_K$  = 'ionisation' or 'edge onset' energy

i.e.  $E < E_K$  no ionisation,  $E > E_K$  there is a finite probability for ionisation (cross-section). Results in an abrupt onset followed by gradual decay as for valence shell ionisation. Measurement of  $E_K$  often sufficient for element identification.

### Cross-section

As before the signal in the edge is a function of scattering angle, collection angle and energy lost.

$$\frac{d^2\sigma}{d\theta dE} = \frac{2e^4}{Em_0v^2(\theta^2 + \theta_E^2)} \cdot \text{GOS}$$

$m_0$  = electron rest mass

$v$  = electron velocity

$\theta_E$  = 'characteristic' inelastic scattering angle =  $E_K/2E_0$

GOS = generalised oscillator strength - represents contribution of each electron energy level that takes part in the energy loss process.

For small  $\theta$  and small integration window above  $E_K$ , GOS is  $\approx$  constant, then:

angular distribution is of form  $(\theta^2 + \theta_E^2)^{-1}$  with a maximum at  $\theta=0$ .

For example, for a 300eV loss @ 100kV we have  $\theta_E \approx 1.5\text{mrad}$  and an average scattering angle of  $5\theta_E$ .

As  $\beta$  (collection angle) increases from zero, signal increases but will saturate at angle  $\approx \sqrt{2}\theta_E$  (about 50mrad for most elements).

For the total cross-section again we must integrate from  $E_K$  to a loss equal to  $E_0$  and for all values of  $\theta$ .

Typically for light elements, e.g. C,  $\sigma_{\text{tot}} \approx 10^{-20} \text{ cm}^2/\text{atom}$  - 2 orders of magnitude smaller than elastic or plasmon cross-section  $\therefore$  edge very weak. Consequently the mean free path is much longer: several microns  $\therefore$  for a 50nm foil only a few electrons will ionise an inner core electron, although many more will be 'diffracted' or interact with valence shell electrons.

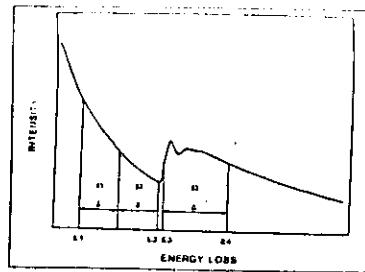
**NB** In practise spectrometer works over finite range ( $\Delta$ ) of  $E$  &  $\beta$   $\therefore$  need to calculate partial cross-section  $\sigma(\beta, \Delta)$ .

### Background Modelling

Experimentally it has been found that the signal decays exponentially and can be fitted to a power law over small energy ranges, i.e.

$$I = AE^{-r} \text{ with } r \text{ in range } (3-5)$$

Thus it is possible to make a log-log plot and determine the slope and intercept. Most typically a least squares fit routine is applied (of varying sophistication) or a simple graphical technique (especially when the spectrum is very noisy).



$$\text{Intensity in edge, } I_K = I_3 \cdot A \cdot \left[ \frac{E_4^{1-r} - E_3^{1-r}}{1-r} \right]$$

where:

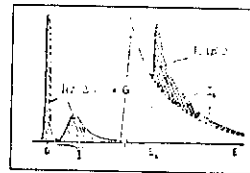
$$r = \frac{2 \log_{10} \left( \frac{I_1}{I_2} \right)}{\log_{10} \left( \frac{E_2}{E_1} \right)}$$

and

$$A = \frac{[(I_1 + I_2)(1-r)]}{[E_2^{1-r} - E_1^{1-r}]}$$

typical fitting windows 30% of  $E_K$ , e.g. C  $E_K = 284\text{eV}$ ,  $\delta \approx 100\text{eV}$ .

### Quantitation



### Modelled

Detected count rate,  $R$ , of edge loss events

$$R = I \cdot N \cdot \sigma$$

$I$  = incident electron flux ( $\text{e}^{-1}\text{m}^{-2}$ )  $N$  = number of atoms contributing to edge, under beam

Assuming collection from 0 to  $2\pi$  and losses from  $E_K$  to  $E_0$  (i.e.  $(E_0 - E_K)$  to  $0\text{eV}$ ).

In practise finite collection angle,  $\beta$  and practical energy integration window,  $\Delta$ .

$$N = \frac{I_K(\beta, \Delta)}{I_l(\beta, \Delta) \sigma(\beta, \Delta)}$$

$I_l$  = intensity in low loss region for same energy window

If know partial cross-section (calculation or experiment) can obtain  $N$

Normally want to know ratio of element wrt another element, in this case it is simply

$$\frac{N_A}{N_B} = \left( \frac{I_A}{\sigma_A} \right) \times \left( \frac{\sigma_B}{I_B} \right)$$

where  $A$  and  $B$  identify the element and  $I$  denotes number of counts. Cross-sections are difficult to calculate to very high accuracy (10% is considered very good).

### Standards

If know composition of similar material and keep same values for  $\beta$  and  $\Delta$ , then ratio of edge integrals for  $A, B$  in unknown and standard gives a quick and accurate composition.

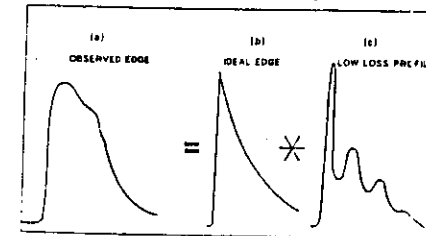
**NB** There are no absorption or fluorescence corrections or detector corrections (in serial spectrometers but not in case of PEELS).

### Plural Scattering

As sample thickness increases so to does the probability of electrons being scattered more than once. The basic quantitation methods assume single scattering. The effect of plural scattering is to re-distribute the counts away from the edge onset. For a large energy integral the counts will be the same but visibility of the edge is reduced (and hence accuracy in fitting the background, etc.). Edges at high losses are more rapidly affected than edges at low losses. Spectrum is the convolution of single scattering spectrum with low loss region. Deconvolution methods can be applied but in general all tend to accentuate any statistical noise in spectrum and weak edges will become lost in the noise. Quantitation equation is then modified to

$$N = \frac{I_K(\beta, \Delta)}{I_0 \sigma(\beta, \Delta)}$$

where  $I_0$  is the incident beam integral without specimen present.



## LIGHT ELEMENT ANALYSIS

What are the "Light elements"?

H, He, Li, Be, B, C, N, O, F, Ne, Na, Mg, Al, Si, .....

What is experimental objective?

Detection      Quantitation      Valence state

### EDS

#### Detection

Fluorescence Yield

Element	$\omega$
B	0.0006
C	0.0027
N	0.0047
O	0.0065

i.e. for oxygen only 0.7% of ionisation events will result in the emission of an x-ray, the rest will give Auger electrons. Compare to Al (4%), Ti (20%), Zn (50%).

Why are any detected at all?

Answer:- large ionisation cross section (cf. EELS)

Detector design -> type of window and SiLi crystal construction.



#### Quantitation

Important parameters:-

- background subtraction
- peak overlap
- detector response
- absorption
- mass loss

### EELS

Detection of primary excitation process - therefore all ionisation events can contribute to EELS spectrum (x-ray and Auger transitions are the de-excitation processes).

#### Detection

See EELS notes.

Note detectability is a function of other elements present.

#### Quantitation

Important parameters:-

- background subtraction
- mass loss

### Beam Induced Decomposition

Many light elements can be lost due to electron beam interactions -> result is a decreasing composition as a function of dose rate and total dose. Accelerating voltage or temperature dependences. May be very significant for oxides, carbides and nitrides and is very rapid for Na and Li containing alloys.

